16th World Conference on Earthquake, 16WCEE 2017
Santiago Chile, January 9th to 13th 2017
Paper N° 882
Registration Code: S-A1463080124

NUMERICAL SIMULATION OF REINFORCED CONCRETE COLUMNS UNDER BIAXIAL CYCLIC BENDING AND VARIABLE AXIAL LOAD

M. Poliotti [1], O. Möller [2], J.P. Ascheri [3] , P.L. Sierra [4]

[1] *PhD Student, IMAE-UNR, poliotti@fceia.unr.edu.ar*
[2] *Professor, CIUNR-IMAE-UNR, moller@fceia.unr.edu.ar*
[3] *Professor, IMAE-UNR, jascheri@fceia.unr.edu.ar*
[4] *PhD Student, IMAE-UNR, sierrapa@fceia.unr.edu.ar*

Abstract

Numerical simulation of reinforced concrete structures is important in the assessment of nonlinear behavior of new and existing structures susceptible to earthquake loads. Columns are subjected in the general case to biaxial bending and varying axial loads during an earthquake and the interaction between these efforts has a strong influence in the nonlinear response, modifying the strength, stiffness and ductility of these elements.

Several numerical models exists nowadays in literature for nonlinear dynamic analysis of beam-column elements that take into account the interaction between bending moments and axial load with different degrees of accuracy and robustness. The best way to test them is by contrast of numerical results with experimental data, but this is not an easy task mainly because laboratory tests involving cyclic biaxial bending with varying axial load are rare in literature.

In this work a flexibility-based element with fiber discretization of the cross section on each integration point of the Gauss-Lobato integration rule is used in order to reproduce part of an experimental campaign performed by other authors. Euler-Bernoulli's hypothesis is used to calculate deformations of the fibers and material nonlinearity is reproduced by uniaxial laws at each fiber of the cross section. Modified versions of Mander's constitutive law and Menegotto-Pinto's law are used for concrete fibers and reinforcement steel fibers respectively. With this model the nonlinear behavior of four identical cantilever columns subjected to different paths of imposed horizontal displacements that lead to biaxial cyclic bending in conjunction with variable axial load is simulated numerically. Results of the hysteretic behavior obtained by the numerical model and the experimental test data are overlaid and compared.

Comparison shows that the numerical model used in the simulation is able to reproduce the maximum strength and the dissymmetry caused by variations of the axial load, also the general behavior and interaction among cyclic moments and axial load is reproduced. Differences appear in the post-peak response especially softening is quicker in the simulation than the registered response of the tested specimen. Also the peak displacement values obtained by the model are smaller than the measured one. Discrepancies are explained by the limitations and hypothesis of the element and constitutive laws used. Finally further developments to improve the accuracy are proposed.

Keywords: Reinforced concrete columns, fiber-beam model, variable axial load, biaxial cyclic bending.

1. Introduction

Reinforced concrete structures under seismic loads have their columns under the coupled effect of bending cyclic moment and variable axial loads. In particular, corner columns are subjected to biaxial cyclic moments and strong variations of the axial load. These variations are of major importance because the axial load has a strong influence in the strength, stiffness and ductility of the columns. [1]

The study of these elements is vital especially in the assessment of existing structures that were not designed using the current performance based codes. Several numerical models are available nowadays in literature that can reproduce with different levels of accuracy the complex response of reinforced concrete beams or columns but calibration with experimental data of this kind of elements is not an easy task due to the lack of experiments where the variations of the axial load is taken into account. [2, 3, 4]

In this paper part of the experimental campaign driven by Rodrigues *et al* [2], where a group reinforced concrete columns were tested under the effects of biaxial cyclic bending and variations of the axial load, is reproduced numerically in order to test the capabilities and limitations of a flexibility based fiber-beam element with Gauss-Lobato integration rule and Euler-Bernoulli's kinematic hypothesis [5, 6, 7]. Material nonlinearities are reproduced by uniaxial laws on each fiber of the cross section, Mander's [8, 9] constitutive law is used for concrete fibers and Menegotto-Pinto [10, 11] for the case of steel fibers. Numerical and experimental results are compared and the limitations of fiber-beam element and the corresponding constitutive laws are discussed.

2. Description of the experimental tests

The experimental campaign that is numerically simulated in this work was carried out by Rodrigues *et al* [2] making focus in the effects of variations in the axial load with biaxial cyclic bending. A total of 6 identical cantilever columns were tested under different paths of horizontal imposed displacement history with concomitant variations of the axial load. The main features of the test can be seen in Fig. 1.

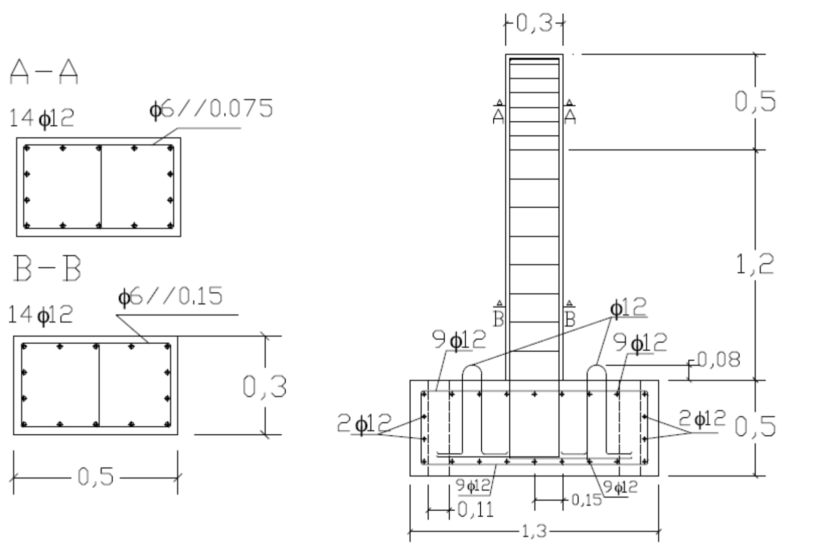

Fig. 1 – Reinforcement and dimensions of the experimental specimens (Rodrigues *et al* [2])

The horizontal top displacements were introduced by two orthogonal actuators attached to the column in the last 20 cm leaving 150 cm of free height to the column. The axial load was introduced by a vertical actuator with a special sliding device in order to reduce the friction between the column and the actuator.

The specimens were tested with different horizontal displacement paths, the first two were uniaxial paths following the strong and weak directions of the cross section. The other four were tested following a rhomboidal path, a diagonal path (45º between the strong and weak direction), a quadrangular path and finally a circular path. Each path was applied in increasing nominal peak displacement levels (3, 5, 10, 4, 12, 15, 7, 20, 25, 30, ⋯, 80mm) with three cycles on each demand level. The axial load was applied relatively to the history of the strong direction displacement with a mean value of 300 KN (compression) and variations of ±150 KN, reaching its extreme values for the yield displacement (which was previously estimated) and being constant for greater displacements values, see Fig. 2. The top displacements and applied loads were measured in order to be able to draw the force displacement hysteretic behavior in both strong and weak directions of the columns. A more extensive detail of the experimental campaign and results can be found in Rodriguez *et al* [2].

Fig. 2 – Applied axial load related to the strong direction displacement (*)

Only the four specimens with biaxial horizontal paths are taken into account in this work to make focus in the biaxial bending behavior with variable axial load.

3. Numerical simulation

3.1 General description of the model

Numerical simulation of the four columns is made using a single 3D fiber-beam element with three integrations points for the Gauss-Lobato integration rule. Each integration point the cross-section of the column is meshed with 150 concrete fibers and 14 steel fibers, Fig. 3.

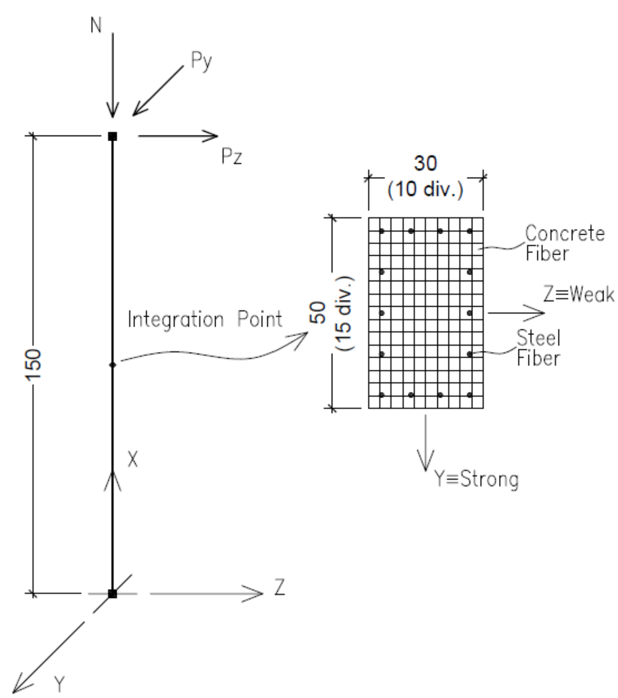

Fig. 3 – Characteristic and mesh of the simulation

The base node has his 6 degrees of freedom fully restricted and at the top node of the element only displacements in the Y and Z directions are restricted. Horizontal displacements are imposed at the top node on each restricted direction following the same history path that in the experimental campaign. Varying axial load was introduced as a concentrated load at the top of the element following the load history of the experimental campaign.

Nonlinear pseudo dynamic analysis (mass and damping of the element are considered null) is performed using the software DINLIES, Möller [12]. Step by step Newmark's integration method is used in order to solve the dynamic equations, and classical Newton-Raphson method is used for the nonlinear problem.

In the following the element formulation and material models and properties are described.

3.2 Fiber-beam model

The numerical solution is obtained using a 3D flexibility based element with fiber discretization on each integration point of the Gauss-Lobato integration rule. This model was first introduced by Taucer *et al.* [5] and implemented by Möller *et al.* [7].

Fiber beam discretization of the cross section at each integration point, Fig. 4, permits to capture the interaction between axial force and bending moments by means of a kinematic hypothesis, in this case Euler-Bernoulli´s hypothesis is taken into account. At the sectional level the process begins with a new set of sections generalized deformations, axial elongation and both bending curvatures. Shear and torsion are taken into account in an uncoupled elastic way in order to assure the equilibrium of the beam. With this deformations and the EB kinematic hypothesis axial deformations on each fiber are calculated as can be seen in Eq.1.

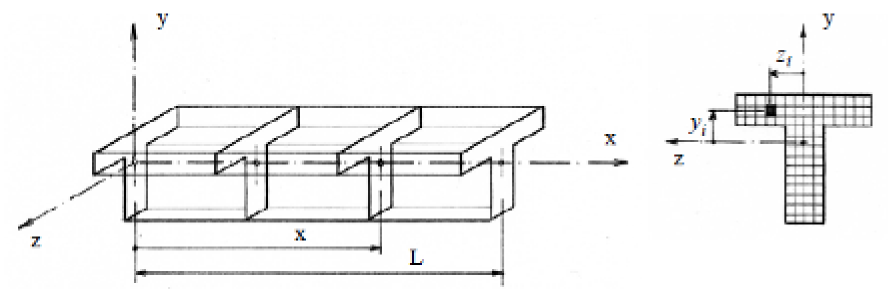

Fig. 4 – Integration points and fiber discretization (Möller *et al* [7])

$$\mathbf{e}(x)=\begin{Bmatrix}\varepsilon_1(x,y_1,z_1)\\ \vdots \\ \varepsilon_i(x,y_i,z_i)\\ \vdots \\ \varepsilon_n(x,y_n,z_n)\end{Bmatrix}=\mathbf{L}(x)\mathbf{d}(x)=\begin{bmatrix}1 & z_1 & -y_1\\ \vdots & \vdots & \vdots\\ 1 & z_i & -y_i\\ \vdots & \vdots & \vdots\\ 1 & z_n & -y_n\end{bmatrix}\begin{Bmatrix}\varepsilon_0(x)\\ \varphi_y(x)\\ \varphi_z(x)\end{Bmatrix} \tag{1}$$

Where $\mathbf{e}(x)$ is the n-vector that contains the axial deformations (ε_i for the i-th fiber) of the n fibers of the cross section, $\mathbf{L}(x)$ is the geometric operator of the cross sections that by means of the plane sections hypothesis relates axial deformations in the fibers with generalized deformations of the cross section $\mathbf{d}(x)$, here only axial elongation ε_0 and bending curvatures φ_Y and φ_Z are taken into account.

Uniaxial material laws are needed in order to calculate the stresses on each fiber, in this case nonlinear constitutive laws are chosen for concrete and steel fibers. Once the stresses were calculated the normal force and bending moments are calculated by simple integration over the section Eq. 2, as well as the rigidity matrix, Eq. 3.

$$\mathbf{D}(x) = \begin{Bmatrix} N(x) \\ M_y(x) \\ M_z(x) \end{Bmatrix} = \begin{Bmatrix} \sum_{i=1}^{n} \sigma_i A_i \\ \sum_{i=1}^{n} \sigma_i A_i z_i \\ -\sum_{i=1}^{n} \sigma_i A_i y_i \end{Bmatrix} \tag{2}$$

$$\mathbf{k}(x) = \begin{bmatrix} \sum_{i=1}^{n} E_i A_i & \sum_{i=1}^{n} E_i A_i z_i & -\sum_{i=1}^{n} E_i A_i y_i \\ & \sum_{i=1}^{n} E_i A_i z_i^2 & \sum_{i=1}^{n} E_i A_i y_i z_i \\ sym. & & \sum_{i=1}^{n} E_i A_i z_i^2 \end{bmatrix} \tag{3}$$

Where $\mathbf{D}(x)$ is the vector of generalized stresses or interior efforts composed by the axial force and both bending moments that are calculated by integration of the normal stresses of each fiber σ_i. Also the rigidity matrix of the section $\mathbf{k}(x)$ is computed by integration of the tangent modulus of each fiber E_i over the cross section.

The element and sectional state determination in nonlinear problems has to be solved in an iterative manner. The process has three iteration levels, at the structural level a load control (classical Newton-Raphson with updated stiffness matrix) method is used, at the element level a displacement control method is used and finally another iteration process is made at the sectional level in order to assure inner equilibrium.

The integrals of the element formulation are performed using the Gauss-Lobato integration rule which has the advantage of including the endpoints of the element where usually the nonlinear behavior concentrates.

Finally the flexibility formulation allows by means of proper force interpolation functions to satisfy the inner equilibrium among sections of the element and also avoids the shear-locking problem.

3.3 Mander´s constitutive law for concrete

The uniaxial constitutive law for confined and unconfined concrete proposed by Mander *et al.* [8] with modifications in the softening traction branch introduced by Martinelli *et al.* [9] is used, Fig. 5. This model allows for cyclic loading using a single backbone curve. Confinement is calculated in base of the transverse reinforcement amount and arrangement.

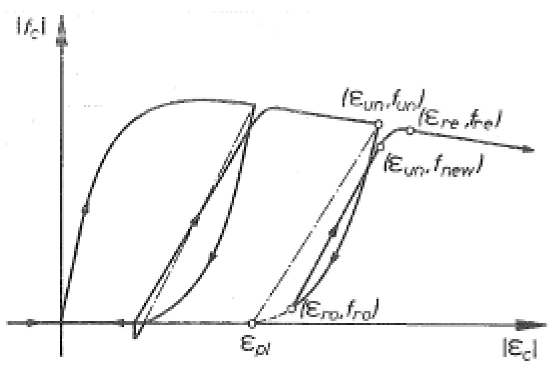

Fig. 5 – Stress strain curve with reloading for concrete fibers (Mander *et al* [8])

Material parameters are estimated using as base the experimental data from Rodriguez *et al.* [2] and also by the transverse reinforcement’s detail that can be seen in Fig. 1. Table 1 summarizes the material parameters used in the numerical simulation.

Table 1 – Material parameters for concrete

f_{cm} [MPa]	f'_c [MPa]	$\rho_{sy} = A_{sy} / (b_c s_h)$	$\rho_{sz} = A_{sz} / (h_c s_h)$	f_{yh} [MPa]	k_e
27.92	22.56	0.00126	0.00113	575.6	0.259

Where f_{cm} and f'_c are the mean characteristic compressive strength of concrete respectively. ρ_{sy} and ρ_{sz} are the volumetric rate of transverse reinforcement on each direction, f_{yh} is the yield stress of the transverse reinforcement and finally k_e is the effectiveness of confinement factor computed in base of the geometry of the section and the reinforcement detail.

3.4 Menegotto-Pinto constitutive law for steel reinforcement

The uniaxial constitutive law for steel proposed by Menegotto *et al.* [10] with modifications in the hardening part proposed by Fronteddu [11] is used in this work. The model reproduces the hysteretic behavior of reinforcement steel taking into account the well-known Bauschinger effect as can be seen in Fig. 6.

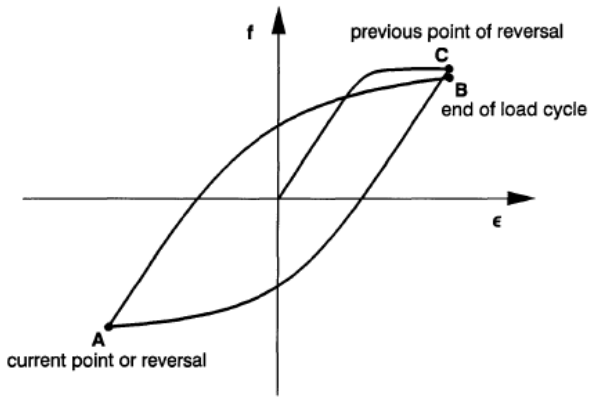

Fig. 6 – Stress and strain curve for steel fibers (Fronteddu [11])

As in concrete, material parameters are deduced using as base the experimental data from Rodriguez *et al.* [2]. Table 2 summarizes the material parameters used in the numerical simulation.

Table 2 – Material parameters for reinforcement steel

f_y [MPa]	E [MPa]	E_p / E	f_{SU} [MPa]	ε_{SU} [%]
575.6	195 980	0.00251	682.8	22.04

Where f_y and f_{SU} are the yield and ultimate stress respectively. E and E_P are the elastic and post yielding modulus respectively, and finally ε_{SU} is the ultimate strain.

4. Results

Results of the numerical simulation of the columns are presented in this section along with the experimental data from Rodriguez *et al.* [2]. The experimental and numerical results are overlaid in the following in order to check differences and similarities between both responses. Numerical simulation is driven until the 30 mm level of nominal peak displacement approximately, after this level numerical response diverges from the experimental one and is not considered in the following analysis.

In Figs. 7 to 10, the hysteretic behavior of the columns is presented by the shear vs drift curve for each horizontal path considered in both strong and weak directions of analysis. In numerical simulations shear is computed as the reaction in top restraints and drift is determined using a free height of 150cm as it was previously described.

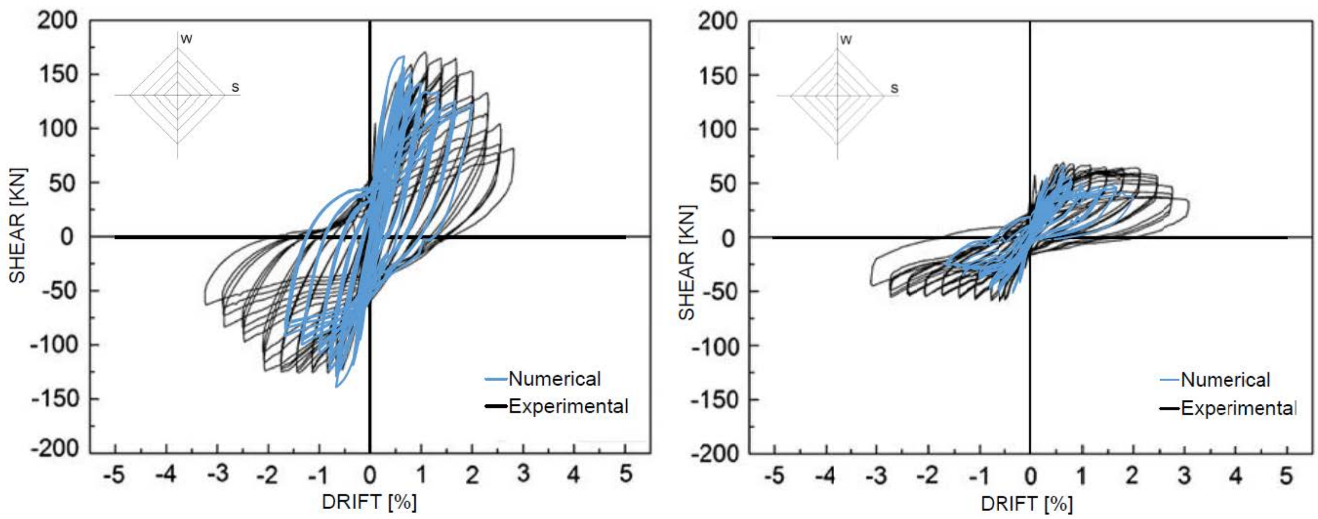

Fig. 7 – Rhomboidal path – (left) Strong and (right) Weak directions (*)

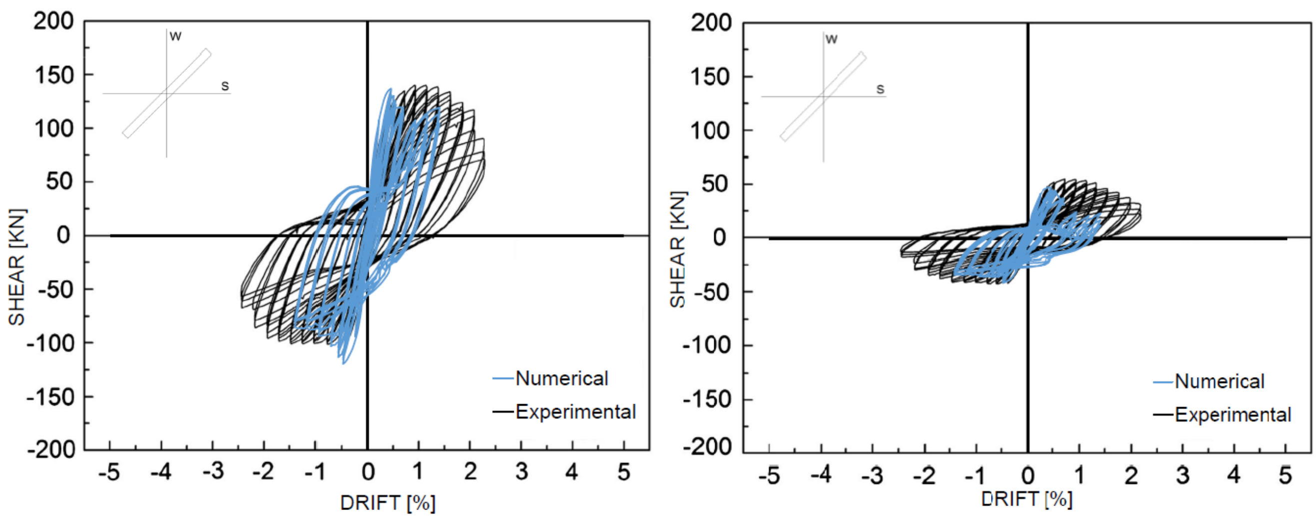

Fig. 8 – Diagonal path – (left) Strong and (right) Weak directions (*)

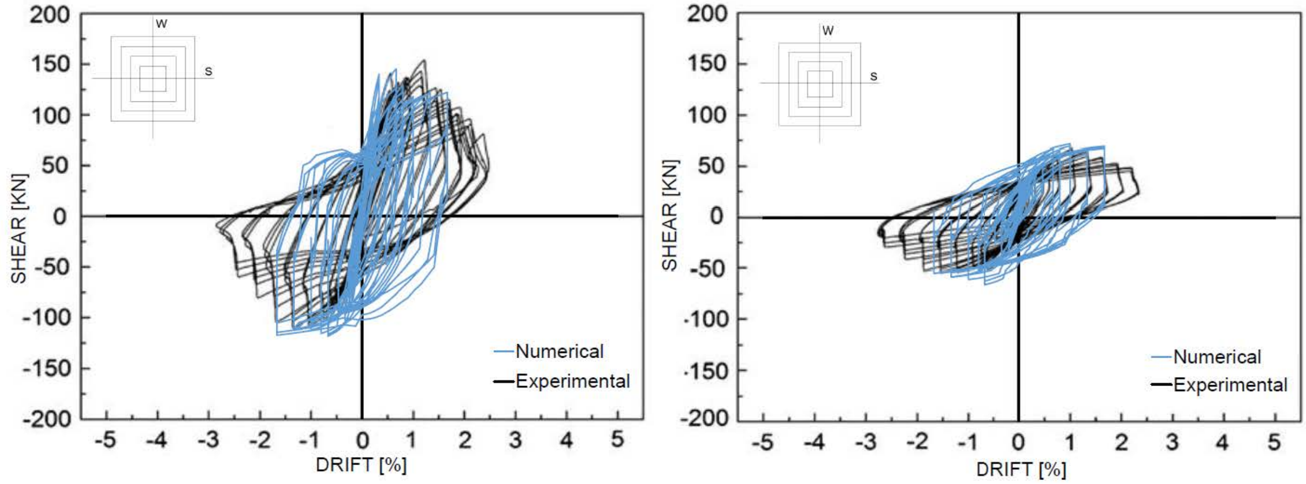

Fig. 9 – Quadrangular path – (left) Strong and (right) Weak directions (*)

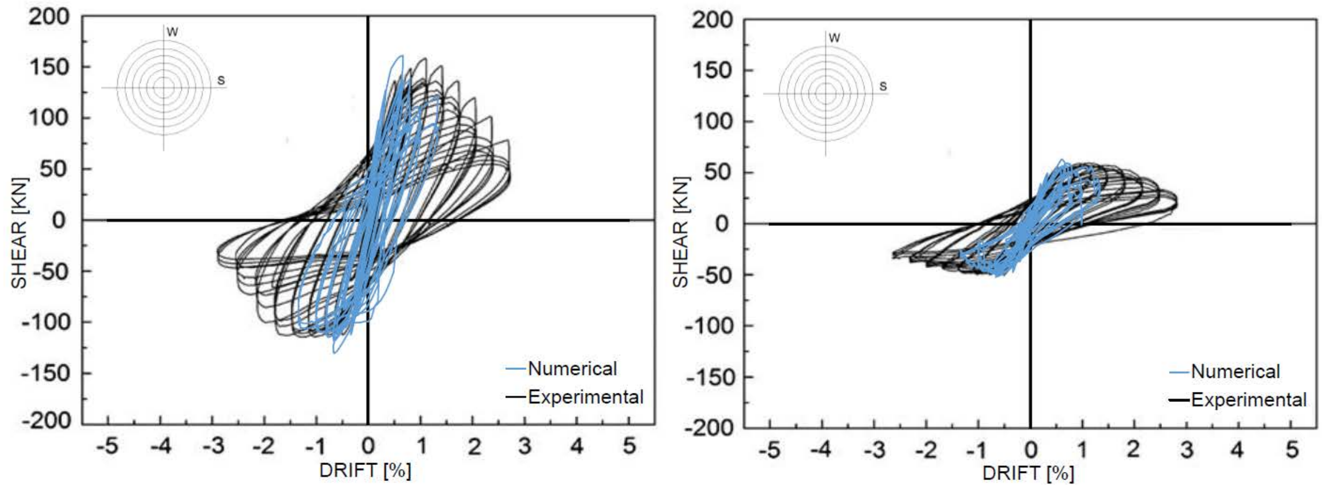

Fig. 10 – Circular path – (left) Strong and (right) Weak directions (*)

Figs. 11 and 12 present the maximum envelopes of the previous shear-drift curves for each column under different load history paths and direction of analysis.

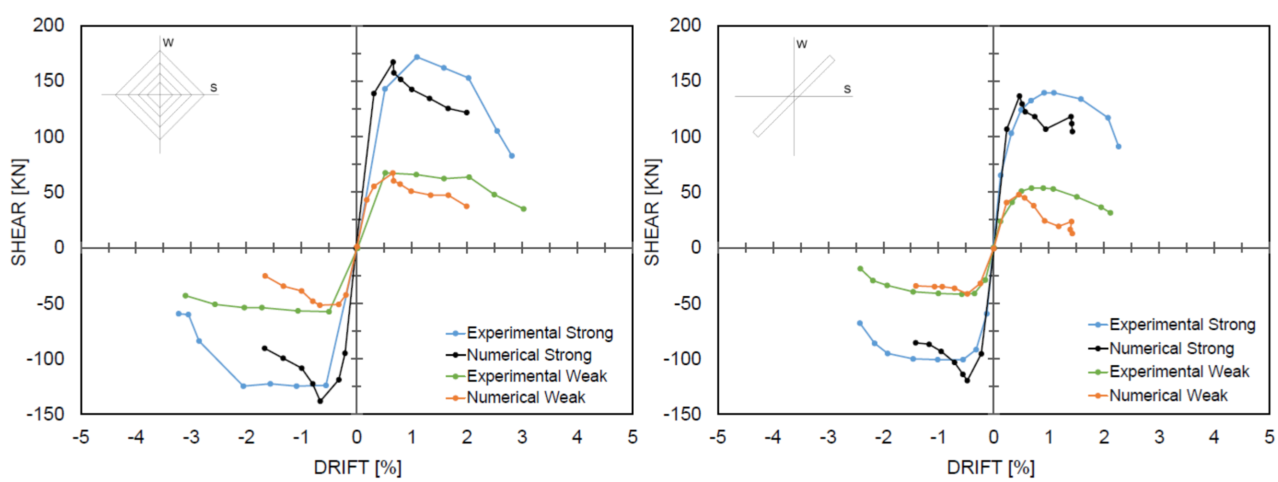

Fig. 11 – Envelopes - (left) Rhomboidal and (right) Diagonal path (*)

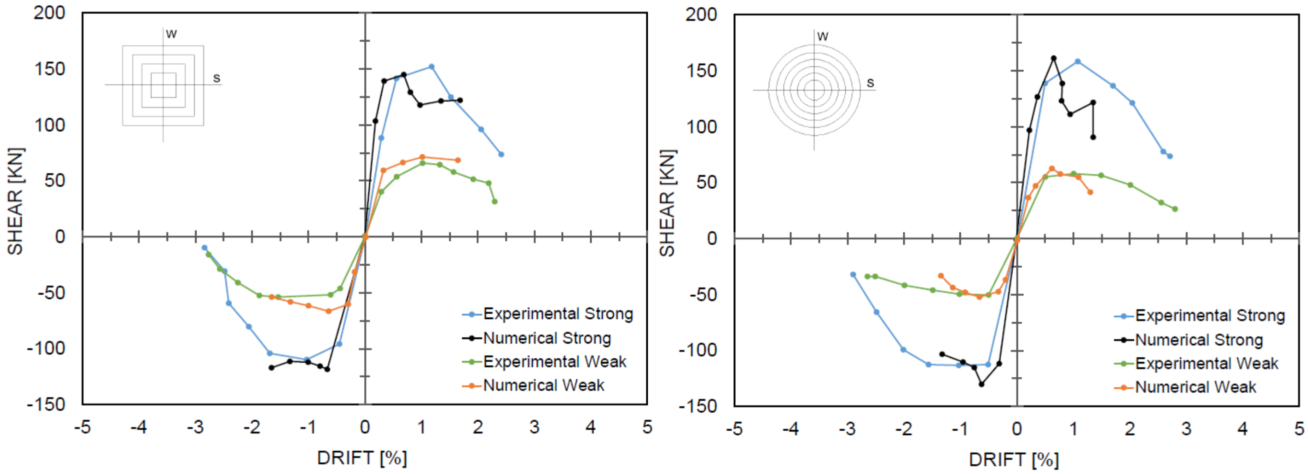

Fig. 12 – Envelopes - (left) Quadrangular and (right) Circular path (*)

(*) Figures were developed using as base the experimental data and figures from Rodriguez *et al.* [2]

5. Comparison and discussion

In this section differences and similarities between the experimental and numerical results are presented. Differences are explained thought the limitations of the fiber-beam model and constitutive laws used in this work and future improvements are identified.

The numerical model presented is able to reproduce the general behavior of the columns in an acceptable way, also the interaction between the varying axial loads and the cyclic bending moments is captured as it can be seen in the hysteretic curves in Figs. 7 to 10. The peak strengths in both weak and strong directions of analysis obtained by the simulation have small differences with the ones obtained in the experimental campaign. Also the dissymmetry in the peak strengths between the positive and negative directions caused by the variations in the axial load is well captured by the model as it can be seen in the envelope curves, Figs. 11 and 12.

The main differences among the experimental results and the numerical response appear in the post-peak response. The numerical model exhibits an abrupt softening after the strength reaches the maximum value. Another difference that can be acknowledged is that near the peak strength takes place for smaller displacements values in the numerical simulation than in the experimental tests. Finally the model is not able to follow the experimental test for high levels of nominal peak displacements. These differences can be, at least partially, explained by the limitations and hypothesis of the element and constitutive models used in the numerical simulation.

The fiber-beam model, as it was already explained, uses the Euler-Bernoulli hypothesis to calculate fiber´s elongations. This hypothesis neglects shear deformations and also neglects inter-fiber equilibrium. Shear deformations are not taken into account in most applications and this hypothesis is valid for slender elements and low level loads, but once diagonal cracking appears the influence of shear deformations increases and cannot be neglected near the peak strength, as it was demonstrated by Bairán [13]. Also, as it was previously remarked, this model considers that each fiber behaves uniaxially and no interaction between fibers is taken into account (inter-fiber equilibrium is violated), also the presence of transverse reinforcement is not considered at the sectional level, this leads to the problem that confinement and the effects of transverse reinforcement have to be reproduced by the constitutive law.

Mander’s constitutive law considers a single and constant backbone curve which is computed for a single confinement pressure. This pressure is calculated by means of the amount and arrangement of the transverse reinforcement and is considered constant all over the nonlinear process. Varying axial load produces variations in the confinement conditions that cannot be reproduced by means of this law. Also in the nonlinear range the dilatancy phenomena modifies the transverse deformations and in consequence modifies the confinement pressure. This constant confinement consideration in addition to the previous mentioned hypothesis of the element may affect the softening branch where the bigger differences between the experimental and numerical responses appear. Also the constitutive law doesn't takes into account the low-cycle fatigue phenomena, which can also be a source of discrepancy.

Other possible cause of error in the numerical simulations is the restrictions used in the bottom node. Full restriction of rotations may not be achieved because of the concentrate rotations that take place when small bond-slipping of the longitudinal reinforcement occurs, this rotations are of major importance when the peak displacement level increases.

Similarities and differences here presented show that this kind of element and constitutive laws can be used with acceptable agreement for nonlinear analysis of reinforced concrete structures, but further developments are needed in order to improve the accuracy especially for large demand levels. At the element level the sectional models presented by Bairán *et al.* [14] Möhr *et al.* [15] showed to be able to reproduced 3D effects and inter-fiber interaction keeping the simplicity of a fiber-beam element framework, in this line a new sectional model and element is being developed. At the constitutive level, more sophisticated equations are available in literature for concrete, plasticity based, damage based, and coupled models have their own advantages and disadvantages, the choice to implement a new constitutive law for concrete for improve the accuracy of the model has to be made making emphasis in the robustness of the model.

6. Conclusions

In this work a flexibility based fiber-beam element with Gauss-Lobato integration combined with Mander's constitutive law for concrete and Menegotto-Pinto law for reinforcement steel was tested by the simulation of an experimental campaign of 4 identical cantilever columns subjected to cyclic bending moments and varying axial loads.

The numerical model showed to be able to reproduce the interaction between cyclic bendings and axial force and also the general response of the columns. Especially the peak strength of the column was well captured and the influence of varying axial load was also reproduced. This leads to the conclusion that this element is suitable for nonlinear analysis of reinforced concrete structures. Although, the simulation exhibits differences with the experimental results particularly after the peak strength was reached, the numerical response showed a quicker softening than the experimental test.

The discrepancies were explained by the hypothesis and limitations of the presented models. The lack of accuracy in the determination of the real confinement state affects the softening branch of the numerical response, also the plane section hypothesis used in the fiber-beam model neglects shear deformations which have an increasing influence after the first diagonal crack takes place.

Further developments were discussed, particularly the development of a new element with sectional analysis capable of reproducing 3D effects without losing the simplicity of beam elements. Also the implementation of more sophisticated constitutive laws for concrete is desirable.

7. References

[1] Poliotti, M., Möller, O., and Ascheri, J.P. (2013): Modelo numérico de elemento de barras discretizado en fibras para columnas sismorresistentes. *Mecánica Computacional* Vol. XXXII, 807-827, AMCA.

[2] Rodrigues, H., Furtado, A., and Arêde, A. (2016): Behavior of Rectangular Reinforced-Concrete Columns under Biaxial Cyclic Loading and Variable Axial Loads." *Journal of Structural. Engineering*, **142** (1), 10.1061/(ASCE)ST.1943-541X.0001345

[3] Rodrigues, H. (2012): Biaxial seismic behavior of reinforced concrete columns. Ph.D. thesis, Univ. of Aveiro, Aveiro, Portugal.

[4] Ceresa, P., Petrini, L., and Pinho, R. (2007): Flexure-shear fiber beam-column elements for modeling frame structures under seismic loading. *Journal of Earthquake Engineering*, ASCE, **11**(1), 46-88.

[5] Taucer, F.F., Spacone, E. and Filippou, F.C. (1991): A fiber beam-column element for seismic response analysis of reinforced concrete structures. *Earthquake Engineering Research Center*, Report Nº EERC 91-17, University of California, Berkeley.

[6] Taylor, R.L., Filippou, F.C., Saritas, A. and Auricchio, F. (2003): A mixed finite element method for beam and frame problems. *Computational Mechanics*, **31**, 192-203.

[7] Möller, O., Quiroz, L., Rubinstein, M (2009): Desempeño numérico de elementos de barra en análisis no lineal estático y dinámico. *Mecánica Computacional* Vol. XXVIII, 587-611, AMCA.

[8] Mander, J.B., Priestley, M.J.N. and Park, R. (1988): Theoretical stress strain model for confined concrete, *Journal of Structural Engineering*, ASCE, **114**(ST8), 1804-1826.

[9] Martinelli, P. and Filippou, F.C. (2007): Numerical simulation of the shaking table test of a seven story RC shear wall structure. ECCOMAS *Thematic Conference on Computational Methods in Structural Dynamic and Earthquake Engineering*, Crete, Greece.

[10] Menegotto, M., Pinto, P.E. (1973) Method of analysis for cyclically loaded reinforced concrete plane frames including changes in geometry and nonelastic behavior of elements under combined normal force and bending. Proceedings IABSE Symp. of Resistance and Ultimate Deformability of Structures Acted on by Well Defined Repeated Loads, Lisbon, 15-22.

[11] Fronteddu, L.F. (1992): Response of reinforced concrete to reverse cyclic loading. Thesis of Ms. of Applied Science, University of British Columbia, Canadá.

[12] Möller, O. (2012): Programa DINLIES. Publicación Interna. Instituto de Mecánica Aplicada y Estructuras, Facultad de Ciencias Exactas, Ingeniería y Agrimensura, Universidad Nacional de Rosario, Argentina.

[13] Bairán, J. (2005): A non-linear coupled model for the analysis of reinforced concrete sections under bending, shear, torsion and axial forces. PhD Thesis, Departament D'Enginyeria de la Construcció, Universitat Politècnica de Catalunya, Barcelona.

[14] Bairán, J. and A. Marí (2006a): Coupled model for the non-linear analysis of anisotropic sections subjected to general 3D loading. Part 1: Theoretical formulation. *Computers & Structures*, **84**, 2254-2263.

[15] Mohr, S. (2010): Nonlinear static and dynamic model for the analysis of reinforced concrete frames under high shear forces. PhD Thesis, Departament D'Enginyeria de la Construcció, Universitat Politècnica de Catalunya, Barcelona.